

**Universitat de Lleida**

Document downloaded from:

<http://hdl.handle.net/10459.1/65847>

The final publication is available at:

<https://doi.org/10.1016/j.solener.2019.02.038>

Copyright

cc-by-nc-nd © 2019 Published by Elsevier Ltd on behalf of International Solar Energy Society.



Està subjecte a una llicència de [Reconeixement-NoComercial-SenseObraDerivada 4.0 de Creative Commons](https://creativecommons.org/licenses/by-nc-nd/4.0/)

1 **Effects of sodium nitrate concentration on thermophysical properties**  
2 **of solar salts and on the thermal energy storage cost**

3 Melanie Durth<sup>1</sup>, Cristina Prieto<sup>1,2,\*</sup>, Alfonso Rodríguez-Sánchez<sup>1</sup>, David Patiño-Rodríguez<sup>3</sup>,  
4 Luisa F. Cabeza<sup>4</sup>

5 <sup>1</sup>Abengoa Energia, c/ Energía Solar 1, 41012 Sevilla, Spain

6 <sup>2</sup>Departamento de Ingeniería Energética, Universidad de Sevilla, Camino de los Descubrimiento s/n,  
7 41092 Sevilla, Spain

8 <sup>3</sup>Facultad de CC Económicas y Empresariales, Universidad de Sevilla, Av. Ramón y Cajal, 41018 Sevilla,  
9 Spain

10 <sup>4</sup>GREA Innovació Concurrent, Universitat de Lleida, Edifici CREA, Pere de Cabrera s/n, 25001 Lleida,  
11 Spain

12 \*Corresponding author: lcabeza@diei.udl.cat

13  
14 **Abstract**

15  
16 Thermal energy storage (TES) systems are key components of concentrating solar power plants  
17 in order to offer energy dispatchability to adapt the electricity power production to the curve  
18 demand. Nitrate molten salts are the storage media used today in concentrated solar power  
19 plants. They are also used as heat transfer fluid (HTF) in the molten salt tower (MST)  
20 technology. Traditional MST plants work in the temperature range of 240-565°C using the so-  
21 called *solar salt*, a mixture of 60-40wt.% of NaNO<sub>3</sub> and KNO<sub>3</sub>. This study wants to optimize  
22 the thermal energy storage cost of the solar concentration technology by analysing different  
23 mixtures of solar salts, using different percentages of NaNO<sub>3</sub> and KNO<sub>3</sub> in the mixture. The new  
24 mixtures seek a reduction in the cost of the storage material while optimizing its physical and  
25 chemical properties. The study shows how an increase in the proportion of sodium nitrate for a  
26 new binary solar salt to 78-22wt.%, produces an increase in the heat capacity of the mixture by  
27 reducing the necessary inventory of salts in the system. However, the new salt presents an  
28 increase in the melting point, going from 240°C to 279°C, which makes the operation of the  
29 system difficult. The impact on the cost of this optimization in the performance of a commercial  
30 plant was analysed. The plant chosen to evaluate the impact is a tower technology plant with 85  
31 MWe power and 13 hours of storage. The study shows a LCOE reduction of up to 0.6% for the  
32 new mixture with higher sodium nitrate.

33  
34 **Keywords:** molten salts; thermal energy storage (TES); Levelized Cost of Energy (LCOE)

## 36 1. Introduction

37

38 The competitive advantage of concentrated solar plants (CSP) is the capability of overcoming  
39 the natural intermittencies of the sun with thermal energy storage (TES) to produce electricity  
40 continuously beyond daylight hours [1]. Current CSP power plants use nitrate molten salts as  
41 their storage media and, depending of the technology, also as their heat transfer fluid (HTF) in  
42 molten salt tower (MST) designs. Traditional nitrate MST power plants work in the 240-565°C  
43 temperature range using the so-called *solar salt*, a 60-40wt.% mixture of  $\text{NaNO}_3$  and  $\text{KNO}_3$ .

44

45 It is well known that the range of operation temperature is not the only criterion to evaluate TES  
46 and HTF medium [2]. Thermal physical properties are also important, such as viscosity, density,  
47 specific heat capacity, and thermal diffusivity, because they are the basic and essential  
48 engineering data. These thermal properties of solar salt 60:40 are well described in several  
49 papers [2–6]. Currently many research groups are working on new mixtures that increase the  
50 thermal stability of the salts, in order to enhance the efficiency of the power cycle [7]. There are  
51 also several groups working on the search for new mixtures that have a lower melting  
52 temperature to save operating costs [2,8]. However, the impact of differing concentrations of  
53  $\text{NaNO}_3$  and  $\text{KNO}_3$  may optimize the thermal properties from the used data.

54

55 To investigate the effects of different mixture of nitrate salts on its thermal properties, seven  
56 mixtures of  $\text{NaNO}_3/\text{KNO}_3$  were selected varying the content of  $\text{NaNO}_3$ . This research examines  
57 the behaviour of these different molten nitrate mixtures, with the goal of improving the solar  
58 salt used currently as an energy storage fluid in CSP plants. These mixtures, which contain  
59 different weight percentages of  $\text{NaNO}_3$  and  $\text{KNO}_3$ , could exhibit better physical and chemical  
60 properties than the solar salt currently used.

61

62 The melting points, heat capacities and thermal stability of the mixtures were studied by  
63 differential scanning calorimetry (DSC) and thermogravimetric analysis (TGA). TGA  
64 experiments provide a good first approach to understand the thermal stability of new salt  
65 mixtures. In these experiments, a small sample of the salt is heated in an open crucible at  
66 ambient pressure with overflow of the cover gas to measure the mass evolution with time and  
67 temperature. These tests are usually employed to estimate the kinetics of the thermal  
68 decomposition reactions and, from there, estimate a reliable maximum operation temperature  
69 for a given process. To determine the specific heat, tests are carried out with a DSC. These tests  
70 measure the temperature difference between a sample and a reference material (thermal,  
71 physical and chemically inert) in function of time or temperature (sample is subjected to a  
72 temperature program in a controlled atmosphere). The specific heat is the most important

73 property to calculate the inventory of salts necessary for the storage system. A precise  
74 measurement of this property is critical in the design of commercial plants. The methodology  
75 has been optimized in this study using a conventional DSC and a modulated DSC.

76

77 Next, the levelized cost of energy will be used to calculate the potential benefit that the use of  
78 the new higher sodium concentration salts compared with the used today *solar salt*.

79

## 80 2. Material and methods

81

### 82 2.1. Materials

83

84 All the tests of binary mixtures of NaNO<sub>3</sub> and KNO<sub>3</sub>, were done with pure salts from SQM®.

85 The chemical compositions of the sodium and potassium nitrate used for the experimental  
86 analysis developed are included in Table 1.

87

88 **Table 1. Chemical composition of pure NaNO<sub>3</sub> and KNO<sub>3</sub> from SQM (weight%)**

| <b>Purity/Impurities</b> | <b>NaNO<sub>3</sub></b> | <b>KNO<sub>3</sub></b> |
|--------------------------|-------------------------|------------------------|
| Purity (%)               | 99.5 min                | 99.6 min               |
| <i>Chloride (%)</i>      | 0.1 max                 | 0.1 max                |
| <i>Magnesium (%)</i>     | 0.02 max                | 0.01 max               |
| <i>Nitrite (%)</i>       | 0.02 max                | 0.02 max               |
| <i>Sulfate (%)</i>       | 0.10 max                | 0.05 max               |
| <i>Carbonate (%)</i>     | 0.10 max                | 0.02 max               |
| <i>Moisture (%)</i>      | 0.1 max                 | 0.1 max                |

89

### 90 2.2. Mixtures preparation

91

92 The binary mixtures studied are presented in Table 2. Before any analysis, it is important to  
93 dehydrate the samples in order to measure thermal characteristics of salts without bounded  
94 water [9]. Therefore, the samples were prepared first, heating at 300 °C the base salts during 20  
95 min, we poured in a mortar, crushed and kept separately in a dry box. Each mixture was done in  
96 the same way. The base salts were mixed in the corresponding weight concentration. The  
97 mixture was heated at 400°C for 20 minutes and mixed manually with a stick. The mixture was

98 then poured in a mortar, crushed until a fine powder and kept in a dry box. Before each thermal  
99 measurement, the mixture was heated at 200°C during more than 10 hours.

100

101

**Table 2. Mixtures tested in the experiment campaign**

| Mixture number | wt.% NaNO <sub>3</sub> | wt.% KNO <sub>3</sub> |
|----------------|------------------------|-----------------------|
| 1              | 0                      | 100                   |
| 2              | 20                     | 80                    |
| 3              | 40                     | 60                    |
| 4              | 55                     | 45                    |
| 5              | 60                     | 40                    |
| 6              | 80                     | 20                    |
| 7              | 100                    | 0                     |

102

### 103 2.3. Analytical methods

104

105 The heat capacity ( $C_p$ ) measurements were carried out with a DSC2 from Mettler Toledo. The  
106 DSC technic measures the heat capacity by heating a sample and measuring the difference  
107 between the heat flows from the sample (mixture in crucible) and a reference (empty crucible)  
108 as function of temperature. Samples are placed in a 40  $\mu$ L aluminum crucible with a small hole  
109 on the tap. The heat capacity is calculated from heat flow values of three different  
110 measurements: blank (two empty crucibles), sapphire (crucible with sapphire disc and empty  
111 crucible), and sample (crucible with sample and empty crucible).

112

113 The DSC method shows imprecision due to the high level of deviation, around 10% RSD. The  
114 Relative Standard Deviation (RSD) was reduced in this study working in other parameters, such  
115 as the blank and sapphire reference, the crucible position on the sensor and the sample contact  
116 on the bottom of the crucible. The measurements of the blank, sapphire, and different mixtures  
117 (called pack) were performed in immediate succession to be sure that the measurements have  
118 the same imprecision and reference.

119

120 In order to avoid salt creeping out of the crucible, the sample crucibles were prepared with the  
121 salt crushed in a fine powder and a maximum of 10 mg of salt is placed in each crucible.  
122 Furthermore, to ensure as much as possible the same contact of the salt on the bottom of the  
123 crucible, the samples are measured only one time. Once the salt was melted inside the crucible,  
124 by surface tension, the salt goes on the walls of the crucible and the contact of the bottom of the  
125 crucible is not the same. These change of contact leads to high imprecision in  $C_p$  measurement.

126 Finally, crucibles were placed manually in the DSC. The authors of this paper observed that the  
127 blank placed manually in the DSC showed an error of only 5% while a blank placed with a DSC  
128 robot showed an error up to 10%. The conditions to test and measure the heat capacity of the  
129 sample were as follow. In an atmosphere of N<sub>2</sub> at 50 mL/min, the following ramp was  
130 programmed: isothermal ramp at 370°C for 5 minutes, dynamic ramp at 20 K/min from 370°C  
131 to 500°C, and isothermal ramp at 500°C for 3 minutes. Entire packs are measured 12 times and  
132 important mixtures as pure KNO<sub>3</sub>, the eutectic (55wt.% NaNO<sub>3</sub>), the solar salt (60wt% NaNO<sub>3</sub>),  
133 and pure NaNO<sub>3</sub> were measurement more times. Table 3 shows the number of measurement for  
134 each mixture.

135

136

**Table 3. Number of measurements for each mixture.**

| Mixture                     | Number of DSC measurements |
|-----------------------------|----------------------------|
| 1 (Pure KNO <sub>3</sub> )  | 17                         |
| 2                           | 12                         |
| 3                           | 12                         |
| 4 (eutectic)                | 19                         |
| 5 (solar salt)              | 29                         |
| 6                           | 12                         |
| 7 (pure NaNO <sub>3</sub> ) | 18                         |

137

138

139 Modulated DSC is interesting compared to conventional DSC because it does not need a blank  
140 in the methodology. The technic consists in introducing a modulation in temperature according  
141 to a sinusoidal function around a constant temperature during a certain time. In this way, the  
142 reversible C<sub>p</sub> is calculated from the amplitude of the modulated signal of heat flow according to  
143 the following relation:

144

$$145 \text{Rev}C_p = \frac{\text{Heat\_flow\_amplitude}}{\text{Heating\_rate\_amplitude}} * KC_p \quad \text{Eq. 1}$$

146

147 where KC<sub>p</sub> is a calibration constant, which depends on the equipment and is calculated by the  
148 mean of a reference line. In this case, sapphire is the reference line. If there is no thermal event,  
149 the reversible C<sub>p</sub> is zero whereas when modulating the temperature, the reversible C<sub>p</sub>  
150 corresponds to the conventional C<sub>p</sub>. Experimental conditions were those described in the ASTM  
151 E2761-09 standard. The modulation programmed had 0.6°C temperature amplitude and 60 s  
152 frequency around the mean temperature, 450°C. The mean temperature was maintained for 30

153 minutes to allow the stabilization of the heat flow signal and be sure of the precision of the  
154 measurement.

155

156 In order to analyze the peak transition of each mixture, the heat flow was measured from  
157 170°C to 390°C with a heating ramp of 20°C/min, using the DSC described above. For each  
158 mixture, the measurement was done three times to validate the results. The latent heat and  
159 the melting temperature of the salt mixtures were calculated with the Mettler Toledo  
160 software. The latent heat was calculated by integrating the area under the heat flow curve in  
161 which the melting temperature was defined as the onset temperature. Only the solid-liquid  
162 phase transition was investigated in order to know the minimum working temperature in a  
163 CSP plant.

164

165 The stability temperature was measured by thermogravimetric analysis (TGA). The equipment  
166 is the same as a DSC but the sensor is connected to an ultra-sensitive balance and allows  
167 measuring the mass change of the sample at any moment, when the sample is submitted to a  
168 temperature isothermal or dynamic ramp. In that case the interest is to measure the temperature  
169 when the sample lost 3% of its total initial mass. The thermal ramp programmed is 20°C/min  
170 from 400°C to 900°C.

171

## 172 **3. Results**

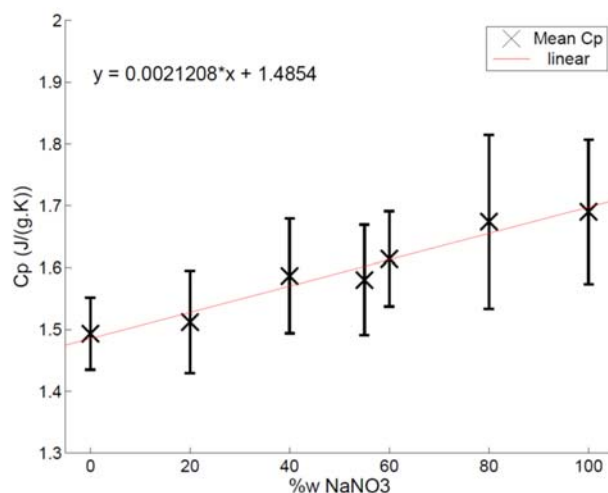
173

### 174 **3.1. Specific capacity results with conventional DSC**

175

176 The mean value of each mixture was calculated in the temperature range between 380°C and  
177 485°C and the mean over all the samples of the same mixture (Table 3). The mean value of  $C_p$   
178 (with its associated error) versus the mixture composition is represented in Figure 1. It is  
179 interesting to note that the points follow a line.

180



181  
182 **Figure 1. Heat capacity of each mixture composition with conventional DSC.**

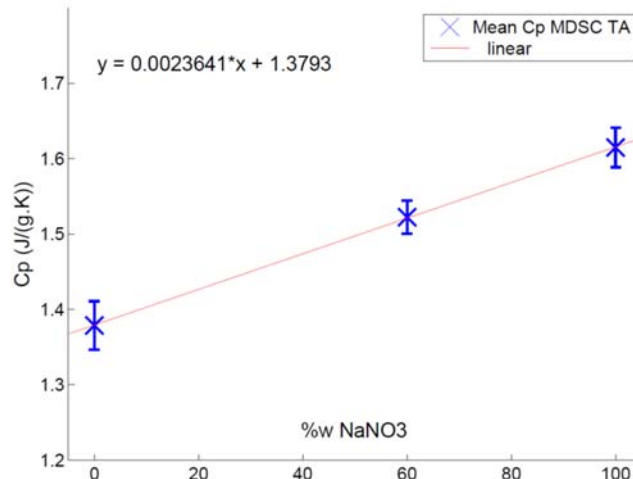
183  
184 Thanks to the corrections followed in the methodology and described in the methodology  
185 section, it was possible to reach a RSD below 8.4% for all the measurement and a mean RSD of  
186 5.8%, which is a very good precision for this equipment (Table 4).

187  
188 **Table 4. Results of heat capacity and RSD associated for all the binary mixtures studied, when**  
189 **using conventional DSC.**

| NaNO <sub>3</sub> (wt.%) | Cp (J/g·K) | RSD (%) |
|--------------------------|------------|---------|
| 0                        | 1.4934     | 3.8     |
| 20                       | 1.5123     | 5.4     |
| 40                       | 1.5867     | 5.8     |
| 55                       | 1.5802     | 5.6     |
| 60                       | 1.6141     | 4.7     |
| 80                       | 1.6739     | 8.4     |
| 100                      | 1.6900     | 6.9     |

190  
191  
192 **3.2. Specific heat capacity results with modulated C<sub>p</sub> methodology**

193  
194 Figure 2 presents the mean C<sub>p</sub> value for the mixture composition. It is interesting to note that,  
195 again, the points follow a line. With this modulated technic, the linearity is confirmed and  
196 shows the same slope as conventional DSC. The modulated technic is much more precise than  
197 conventional DSC methodology, with a maximum RSD of 2.3% (Table 5).



199

200

**Figure 2. Heat capacity versus mixture composition with modulated DSC.**

201

202

**Table 5. Results of heat capacity values and RSD associated when using modulated DSC.**

| NaNO <sub>3</sub> (wt.%) | Cp (J/g·K) | RSD (%) |
|--------------------------|------------|---------|
| 0                        | 1.3788     | 2.3     |
| 60                       | 1.5224     | 1.4     |
| 100                      | 1.6149     | 1.6     |

203

204

Both methods to determine the heat capacity present similar trends that follow the mixing law.

205

According to these results, a salt with higher concentration of sodium nitrate will have higher

206

heat capacity. This  $C_p$  increase will have a positive impact in the solar plant cost, reducing the

207

storage size and the total salt mass flow required.

208

### 209 3.3. Melting point and heat of fusion results

210

211

Table 6 shows the results of the melting point and heat of fusion from the DSC analysis. Both

212

onset and endset values are given, since both are used to give the melting temperature of storage

213

materials. It can be seen that the melting temperature is maximum for the pure materials (being

214

higher for NaNO<sub>3</sub>) and it decreases until a minimum for the mixture known as solar salt

215

(60wt.% NaNO<sub>3</sub> and 40wt.% KNO<sub>3</sub>). Figure 3 shows the results of melting temperature with

216

those from Janz et al. [10]. On the other hand, the melting enthalpy of the increases when

217

increasing the amount of KNO<sub>3</sub> and, as expected, follows the law of mixtures.

218

219

220

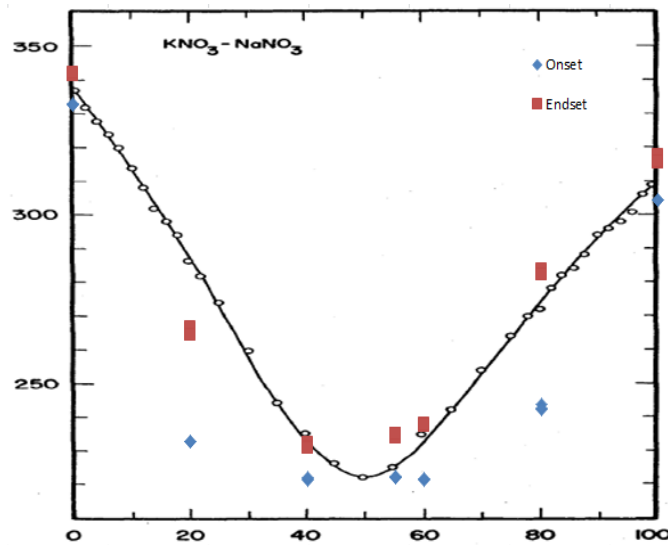
221

**Table 6. Results of melting temperature and heat of fusion for all mixtures**

| NaNO <sub>3</sub><br>(wt.%) | Onset (°C) | RSD (%) | Endset<br>(°C) | RSD (%) | Enthalpy<br>(J/g) | RSD (%) |
|-----------------------------|------------|---------|----------------|---------|-------------------|---------|
| 0                           | 332.93     | 0.07    | 341.63         | 0.16    | 105.96            | 1.15    |
| 20                          | 233.20     | 0.04    | 265.59         | 0.44    | 102.76            | 0.96    |
| 40                          | 222.04     | 0.11    | 231.82         | 0.30    | 112.31            | 0.83    |
| 55                          | 222.54     | 0.08    | 235.00         | 0.28    | 121.65            | 0.75    |
| 60                          | 221.97     | 0.16    | 238.16         | 0.17    | 123.11            | 1.04    |
| 80                          | 243.25     | 0.35    | 283.26         | 0.29    | 195.73            | 0.72    |
| 100                         | 304.63     | 0.05    | 316.47         | 0.34    | 191.33            | 2.16    |

222

223



224

**Figure 3. Results of the melting temperature if the studied mixtures compared to Janz et al. [10].**

226

227 The measured latent heat for NaNO<sub>3</sub> was 191.3 J/g, which is higher than the existing data  
 228 [11]. Salt mixtures with sodium concentration higher than that of *solar salt* (60:40) present  
 229 higher melting point. In a CSP plant, the use of a storage material with higher melting point  
 230 would involve a potential increment of operational problem due to salt freezing. Table 6  
 231 shows that those mixtures also have a higher melting enthalpy, which would mean the need  
 232 of additional energy to melt the salt mixture when filling the storage tanks during the start-  
 233 up phase.

234

235

236

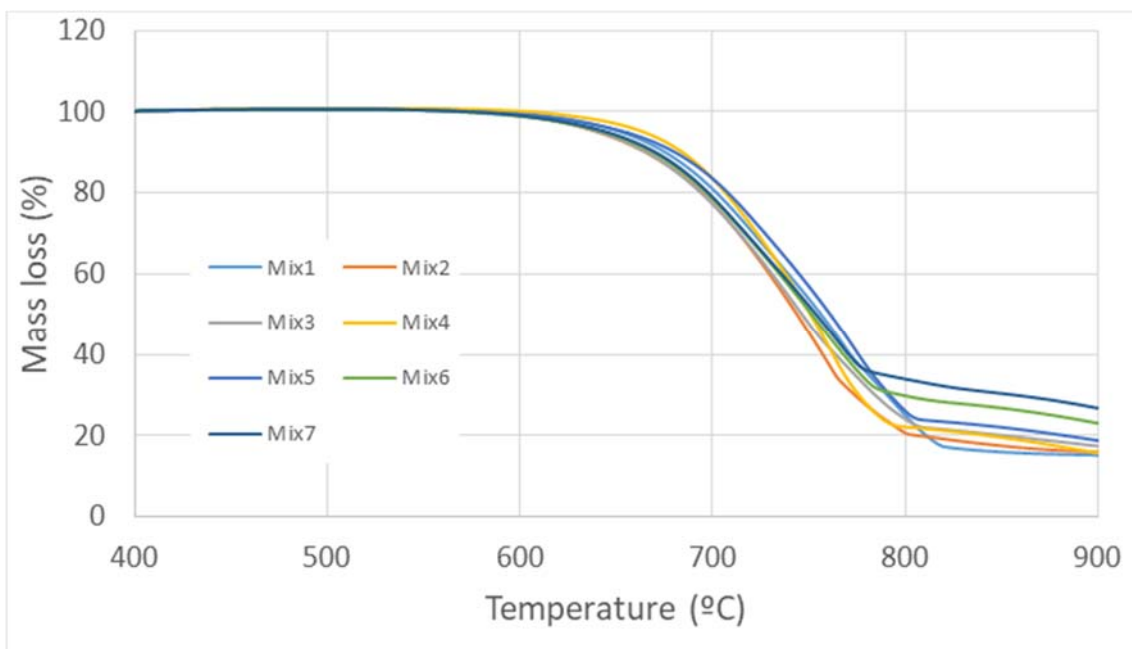
237 **3.4. Thermal degradation**

238

239 Figure 4 presents the % mass loss for each temperature. All seven mixtures show similar  
240 thermal degradation profile. On the other hand, the stability temperature is defined as the  
241 temperature when the sample has lost 3% of its initial total mass. The stability temperature for  
242 each mixture is shown in Figure 5. These measurements show that the stability temperature is  
243 constant for all the mixtures, with a mean value of 646°C and a RSD of 1.7%.

244

245

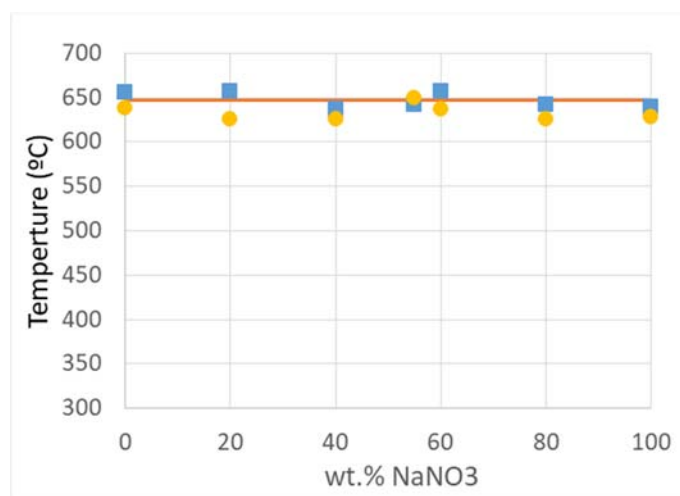


246

247

248

**Figure 4. Mass loss of the studied mixtures.**



249

250

251

**Figure 5. Stability temperature of the studied mixtures.**

252 Thermal degradation is an important parameter to evaluate for the validation of a new salt for  
253 thermal energy storage in CSP plants. Excessive level of degradation can involve the apparition  
254 of new products that could modify the thermal properties of the storage material or even  
255 increase the aggressiveness of the salt in terms of corrosion. The TGA analysis carried out in  
256 this paper does not show any dependence between the thermal degradation and the sodium  
257 nitrate concentration variation.

258

## 259 **4. Economic analysis**

260

### 261 **4.1. Definition**

262

263 Molten salt is the most widespread heat transfer fluid for thermal energy storage in CSP  
264 commercial applications due to its good thermal properties and reasonable cost. Nowadays,  
265 molten salts provide a thermal storage solution for the two most mature technologies available  
266 on the market (e.g. parabolic trough and tower) and could be used as direct and indirect storage  
267 depending of the selected plant philosophy. Both, trough and tower technologies, use double  
268 tank system as thermal storage configurations [1].

269

270 In general, molten salt storage systems offer the possibility to supply electrical production at  
271 constant conditions thanks to maintain the storage material in different tanks when it is charged  
272 or discharged. It also becomes an interesting option as storage material because it has high  
273 energy density per specific volume and very high thermal inertia due to its high heat capacity  
274 and low thermal conductivity. In the state-of-the-art, there are several publications that show the  
275 thermal properties of molten salts, for example *Bauer et al.* [12] makes a good comparison of  
276 the different correlations. The optimization of the thermal properties of molten salt allows like  
277 the design of storage systems with minimum thermal losses that increases global efficiency of  
278 the plant or with lower inventory due to the highest heat capacity.

279

280 As shown in the previous sections, an increase in the proportion of sodium nitrate in the binary  
281 solar salt 60/40 produces an increase in the main properties as heat capacity, melting point and  
282 melting enthalpy. Now, the economic impact of the use of salts with higher sodium  
283 concentration salts in a commercial plant is studied. The plant chosen to evaluate this impact is  
284 a tower technology plant with 85 MWe power and 13 hours of storage, that uses solar salt as  
285 HTF and storage medium. A solar tower plant consists of a large field of heliostats, a heat  
286 transfer fluid/steam generation system, and a Rankine steam turbine/generator cycle [13]. The  
287 direct double tank molten salt storage system is used in the thermal energy storage system [1].

288 The economic study is focused on the storage system since it is the component that would have  
 289 the most relevant cost impact. It is taken as an indicator.

290

291 The heat capacity and density increase are considered as the two most important parameters  
 292 because it allows an exponential decrease in the salt flow required and consequently an  
 293 important reduction in the pump consumption. On the other hand, these two parameters  
 294 enhancement will also involve a direct reduction in storage systems, specifically, the heat  
 295 capacity in the molten salt inventory required and the density in the size of the overall storage  
 296 system. Furthermore, due to the manufacturing process, potassium nitrate is usually more  
 297 expensive than sodium nitrate and thus, salts inventory with higher sodium nitrates will be less  
 298 expensive than the one used today.

299

300 On the other hand, higher melting point, viscosity and heat of fusion will impact negatively in  
 301 the plant in different ways. The higher melting point will involve a higher risk of block  
 302 formation due to salt freezing, therefore, the electric heater systems installed in the plant to  
 303 prevent this problem will need to be re-designed. Furthermore, a higher viscosity, more  
 304 significant at lower temperature, will increase the pressure drop associated in the cold part of the  
 305 facility and, consequently, the pump power required. Finally, salts with higher melting enthalpy  
 306 will also involve higher energy consumption during the melting process in the plant start-up  
 307 period.

308

309 Table 7 shows the variation of these main parameters with concentration of sodium nitrate  
 310 concentration. The physical properties ratios for heat capacity, melting point and melting  
 311 enthalpy were obtained from the experimental results showed in the previous sections. The  
 312 correlation for viscosity and density were calculated from data published in Janz et al. [10].

313

314 **Table 7. Correlation of the physical properties considered in the economic evaluation.**

| Property                     | Correlation   | Regression coefficient |
|------------------------------|---|------------------------|
| Heat capacity (kJ/kg·K))     | $y = 0.0021208 \cdot x + 1.4854$                                    | $R^2 = 0.9555$         |
| Melting point (°C)           | $y = -0.0003 \cdot x^3 + 0.086 \cdot x^2 - 5.7096 \cdot x + 343.46$ | $R^2 = 0.9907$         |
| Heat of fusion (kJ/kg)       | $y = 0.03288 \cdot x + 101.65$                                      | $R^2 = 0.8061$         |
| Viscosity (Pa·s)             | $y = -0.8069 \cdot x^2 + 0.0826 \cdot x + 3.3926$                   | $R^2 = 1.0000$         |
| Density (kg/m <sup>3</sup> ) | $y = 0.0218 \cdot x + 1.857$  | $R^2 = 0.9945$         |

315 x= sodium nitrate wt.% in the binary mixture

316

317 The levelized cost of energy (LCOE) is the price at which electricity generated from a specific  
318 source breaks even over the lifetime of the project [14], and can be formulated with:

319

$$320 \quad LCOE = \frac{f \cdot C_{inv} + C_{O\&M}}{E_{net}} \quad \text{Eq. 2}$$

321

322 where  $C_{inv}$  is the first investment cost,  $C_{O\&M}$  the annual operational and maintenance cost and  
323  $f$  indicates the time dependent interest rate. According to Kearney et al. [5], an interest ratio of  
324 0.104 is a representative value for this type of plants.

325

#### 326 **4.2. Variation in the investment cost ( $C_{inv}$ )**

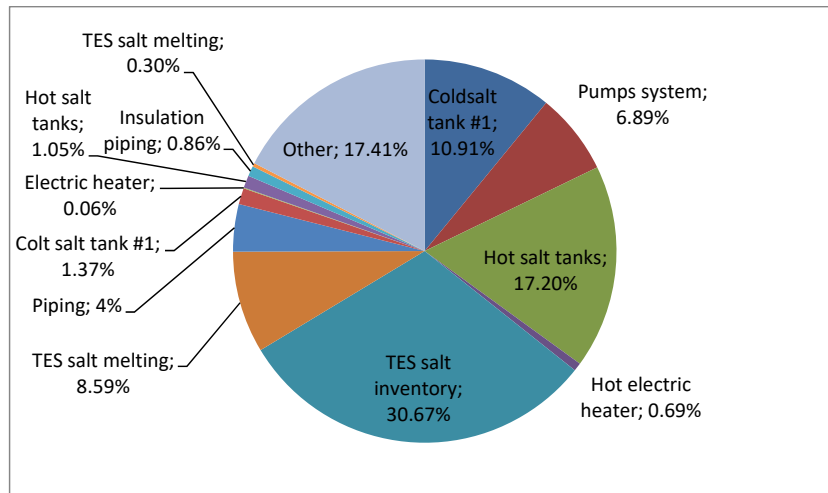
327

328 As it has been mentioned, higher heat capacity and density of the new salts will allow the  
329 reduction of the storage system cost. According to an internal model developed at Abengoa, in a  
330 85 MWe tower plant with 13 hours of storage, the total storage cost represents around 11.03%  
331 of the total cost, corresponding 4.05% to the salt inventory cost and 6.98% to the rest of the  
332 plant; hot and cold tanks, pumps, foundations, structures, insolation, piping associated, salt  
333 melting systems and assembly. Similar values are published by Kolb et al. [15] and by IRENA  
334 [16].

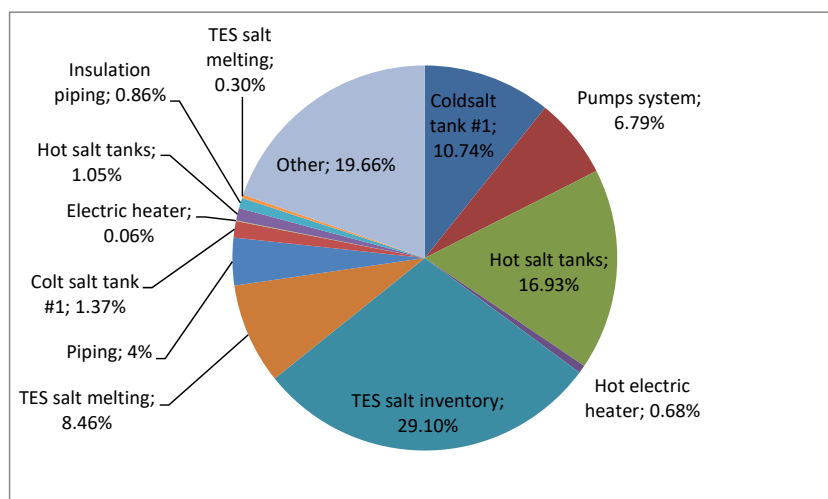
335

336 The investment cost will be also reduced due to the lower cost of the higher sodium  
337 concentration salts in comparison with the *solar salt* (60/40 mixture). In this paper it assumed  
338 that the supply cost of potassium nitrate is 65% higher than the sodium nitrate cost, according to  
339 internal data from salt suppliers of Abengoa. The distribution of cost component and the  
340 variation with the original case is shown in the Figure 6.

341



(a)



(b)

**Figure 6. Comparison of TES cost for (a) solar salt and (b) new mixture molten salt**

342

343

344

345 A reduction cost comparison has been developed in Figure 7. The study releases a molten salt

346 cost reduction up to 5%, and a TES cost reduction up to 2.5%.

347

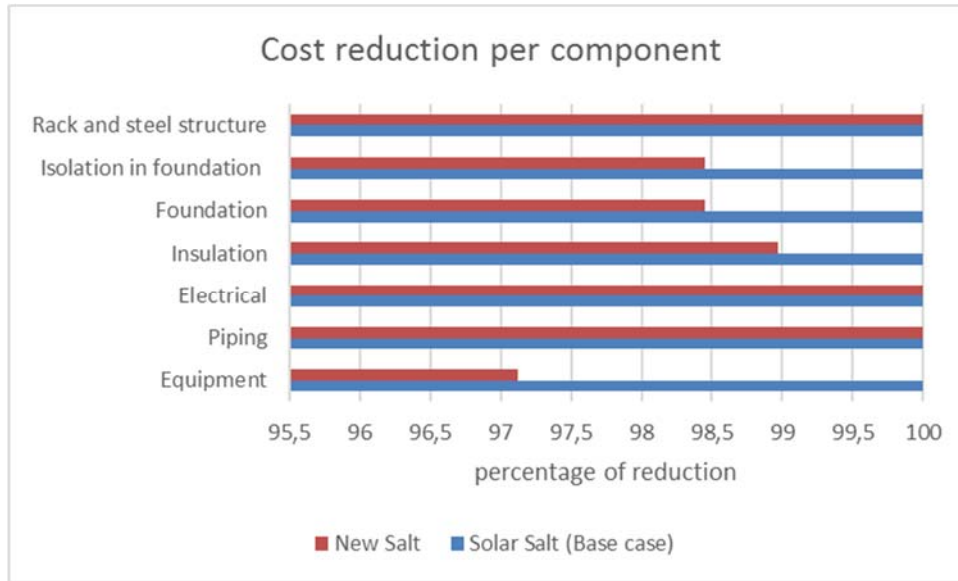


**Figure 7 Comparison of cost reduction per TES component**

348

349

350

351 The cost required to melt the total salt inventory in the base case represents around 0.007% of  
 352 the total investment cost, assuming a natural gas cost of 0.59\$/MWh, initial salt temperature of  
 353 25°C and final melted salt temperature of 360°C. According to the experimental results, higher  
 354 sodium concentration salts will require more energy to be melted, due to the higher  
 355 concentration of sodium nitrate.

356

357 Considering the premises exposed above, the investment cost ( $C_{inv1}$ ) with the new salts  
 358 compared with the investment cost of the case base ( $C_{inv0}$ ) will be:

359

$$360 \frac{C_{inv1}}{C_{inv0}} = 1 + (4.05\%) \left( \frac{C_{p0}}{C_{p1}} - 1 \right) \left( \frac{P_{r0}}{P_{r1}} \right) + (6.98\%) \left( \frac{C_{p0} \rho_{p0}}{C_{p1} \rho_{p1}} - 1 \right) + (0.007\%) \left( \frac{C_{p0} H_{f0}}{C_{p1} H_{f1}} - 1 \right) \quad \text{Eq. 3}$$

361

362 where,  $\frac{C_{p0}}{C_{p1}}$  is the heat capacity ratio,  $\frac{P_{r0}}{P_{r1}}$  the price ratio,  $\frac{\rho_{p0}}{\rho_{p1}}$  the density ratio, and  $\frac{H_{f0}}{H_{f1}}$  the heat of  
 363 fusion ratio.

364

### 365 4.3. Variation in the Net energy produced (Enet)

366

367 As mentioned previously, regarding the energy production, the new salts only will impact in the  
 368 parasitic consumption associated to the pumping system. For this type of plants, the total  
 369 parasitic consumption achieves between the 5% and 10% of the gross electrical production,  
 370 most of this energy is associated to the molten salt pumping system [17,18]. For the plant  
 371 selected, with 85 MWe and 13 hours of storage, internal analysis of Abengoa releases pumping

372 consumption close to 3.6% of the net annual production. Considering this value, the net energy  
 373 produced of a potential plant with higher sodium concentration salt compared with the case base  
 374 will be:

375

$$376 \frac{C_{inv1}}{C_{inv0}} = (3.6\%) \frac{P_{p1}}{P_{p0}} \quad \text{Eq. 4}$$

377

378 where,  $P_{p1}$  and  $P_{p0}$  are the salt pumping consumption of the new plant and the case base  
 379 respectively. The power consumption of the pump  $P_p$ , is formulated as:

380

$$381 P_p = \frac{Q * H}{\tau} = Q^3 f \frac{8L}{D^5 g \pi^2} \quad \text{Eq. 5}$$

382

383 where,  $Q$  is the volumetric salt flow,  $L$  and  $D$  the length and inlet diameter of the pipe,  $g$  the  
 384 gravity, and  $f$  the friction factor that can be assumed for turbulent regimen by the next  
 385 expression:

386

$$387 f = \frac{0.25}{\log\left(\frac{k}{3.7D} + \frac{5.74}{Re^{0.9}}\right)^2} \quad \text{Eq. 6}$$

388

389 where,  $k$  is the absolute roughness of the piping, which for carbon steel pipe is considered 0.045  
 390 mm [19] and  $Re$  the Reynold number, defined by:

391

$$392 Re = \frac{\rho * v * D}{\mu} \quad \text{Eq. 7}$$

393

394 where  $v$  is the velocity trough the piping, and  $\mu$  and  $\rho$  are the viscosity and density of the salt at  
 395 the operation temperature, respectively.

396

397 According to Kearney [20], the volumetric flow of molten salt pumped can be determined in a  
 398 solar plant with:

399

$$400 Q = \frac{Power}{\rho * C_p * \Delta T} \quad \text{Eq. 8}$$

401

402 where  $Power$  is the thermal power absorbed by the salt in the solar receiver,  $\Delta T$ , the increment  
 403 of temperature in the solar receiver and  $C_p$  the average heat capacity between the inlet and outlet  
 404 of the receiver. Considering that the plants objective of this study have the same thermal power,

405 same increment of temperature and similar length of piping for each diameter, Eq. 4 can be  
 406 reformulated as:

407

$$408 \frac{C_{inv1}}{C_{inv0}} = (3.6\%) \frac{\log\left(\frac{k}{3.7D} + \frac{5.74}{Re_0^{0.9}}\right)^2}{\log\left(\frac{k}{3.7D} + \frac{5.74}{Re_1^{0.9}}\right)^2} \left(\frac{\rho_0}{\rho_1} \frac{cp_0}{cp_1}\right)^3 \quad \text{Eq. 9}$$

409 with  $Re_1 = Re_0 \left(\frac{\mu_0}{\mu_1} \frac{cp_0}{cp_1}\right)$  Eq. 10

410

411 **4.4. LCOE**

412

413 LCOE enhancement was calculated considering Eq. 3 and Eq. 9. An annual operational and  
 414 maintenance cost of 17 M\$ [21] and a representative pipe diameter of 22 inches were  
 415 considered.

416

417 Figure 8 shows the LCOE enhancement (in %) considering different salts with sodium nitrate  
 418 concentration between 60% (base case) and 78%. The figure also shows the melting points  
 419 corresponding to each salt, result of the measurements carried out.

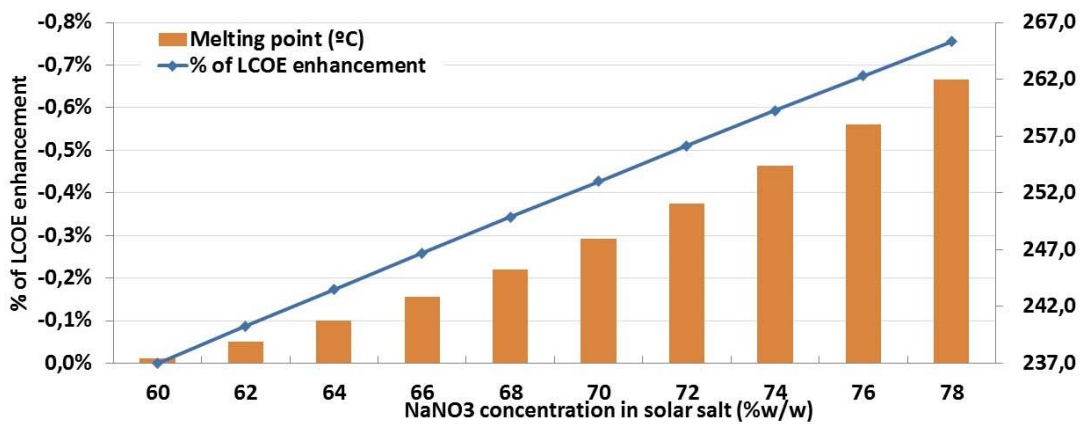


Figure 8. LCOE enhancement and melting point versus the sodium nitrate % in a binary nitrate salt mixture.

420

421 The analysis releases a slight enhancement of the LCOE due mainly to the cost reduction due to  
 422 pumping consumption and the lower storage size required. The negative point is the higher  
 423 melting point of these new salts that will entail higher risk of block formation due to salt  
 424 freezing. To avoid that, the set point of the current electric heater installed in the plant should be  
 425 re-designed. The cost involved to this effect was not included in the present paper and could be  
 426 experimentally analyzed in future studies.

427

428 For future development, the dynamic on the molten salt tank and parasitic consumptions will be  
429 analyzed. A second study is under development where a new performance model is evaluated.

430

## 431 **5. Conclusions**

432

433 This paper describes the impact of the use of salts with higher sodium concentration salts in a  
434 commercial plant performance. Experimental analysis of innovative mixtures of  $\text{NaNO}_3$  and  
435  $\text{KNO}_3$  has been carried out to determine the effect of a higher sodium nitrate concentration in  
436 the main properties required for heat transfer fluids and storage medium in CPS plants. The  
437 plant chosen to evaluate the impact is a tower technology plant with 85 MWe of power and 13  
438 hours of storage.

439

440 Heat capacity, heat of fusion, melting point and thermo-gravimetric analysis of different  
441 composition of sodium nitrate and potassium nitrate mixtures were carried out.

442

443 Two different methods were used to determine the heat capacity, conventional DSC, that use a  
444 reference to determine the  $C_p$  and a modulated DSC, that does not need a blank line. Both  
445 methods present similar trends that follow the mixing law. According to these results, a salt  
446 with higher concentration of sodium nitrate will have higher heat capacity. This increase in  $C_p$   
447 will have a positive impact in the solar plant cost, reducing the storage size and the total salt  
448 mass flow required for the storage.

449

450 Melting enthalpy and melting temperature of the different mixtures considered were also  
451 determined and the results confirmed data from the literature. The main result is that salts with  
452 sodium concentration higher than the *solar salt* (60:40) will have higher a melting point. In CSP  
453 plant, the use of salt with higher melting point will involve a potential increment of operational  
454 problem due to salt freezing. This type of salts also presents a higher melting enthalpy and the  
455 main consequence, compared to the *solar salt*, is the additional energy required to melt the salt  
456 during the tank filling, in the start-up phase.

457

458 The stability temperature of seven different mixtures were measured with TGA, the results do  
459 not show a significant variation of thermal degradation for salts with different concentration of  
460 sodium nitrate.

461

462 These experimental data and other obtained from literature were used to determine the increase  
463 in LCOE of a tower type plant using salt with higher concentration in sodium nitrate salts versus  
464 the current plant using the *solar salt*. The study includes the benefit entailed to the higher heat

465 capacity and density of the new salts, as well as the lower price. On the other hand, also the  
466 negative impact of the higher viscosity and melting temperature were considered. The main  
467 handicap in the use of higher concentration sodium salt is the higher melting point and  
468 consequently, the higher risk of block formation due to salt freezing.

469

470 This preliminary study releases a molten salt cost reduction up to 5%, a TES cost reduction up  
471 to 2.5% and a LCOE reduction up to 0.6% for salts with 78wt.% sodium nitrate, with a melting  
472 point of 279°C. In the new studies, the optimal salt concentration will result from the balance  
473 analysis between the lower LCOE and higher risk associated to a greater melting point.

474

475 These preliminary results encourage continuing with the validation of the new mixtures,  
476 developing a new performance model where dynamic effects and parasitic consumption are  
477 analyzed in more detail.

478

#### 479 **Acknowledgements**

480

481 The work is partially funded by the Spanish government (ENE2015-64117-C5-1-R  
482 (MINECO/FEDER)). Dr. Cabeza would like to thank the Catalan Government for the quality  
483 accreditation given to her research group GREiA (2017 SGR 1537). GREiA is a certified agent  
484 TECNIO in the category of technology developers from the Government of Catalonia.

485

#### 486 **References**

487

- 488 [1] E. González-Roubaud, D. Pérez-Osorio, C. Prieto, Review of commercial thermal  
489 energy storage in concentrated solar power plants: Steam vs. molten salts, *Renew.*  
490 *Sustain. Energy Rev.* 80 (2017) 133–148. doi:10.1016/j.rser.2017.05.084.
- 491 [2] A. Bonk, S. Sau, N. Uranga, M. Hernaiz, T. Bauer, Advanced heat transfer fluids for  
492 direct molten salt line-focusing CSP plants, *Prog. Energy Combust. Sci.* 67 (2018) 1339–  
493 1351. doi:10.1016/j.peccs.2018.02.002.
- 494 [3] D. Kearney, U. Hermann, P. Nava, B. Kelly, R. Mahoney, J. Pacheco, R. Cable, N.  
495 Potrovitza, D. Blake, H. Price, Assessment of a Molten Salt Heat Transfer Fluid in a  
496 Parabolic Trough Solar Field, *J. Sol. Energy Eng. Trans. ASME.* 125 (2003) 170–176.  
497 doi:10.1115/1.1565087.
- 498 [4] U. Herrmann, B. Kelly, H. Price, Two-tank molten salt storage for parabolic trough solar  
499 power plants, *Energy.* 29 (2004) 883–893. doi:10.1016/S0360-5442(03)00193-2.
- 500 [5] D. Kearney, B. Kelly, U. Herrmann, R. Cable, J. Pacheco, R. Mahoney, H. Price, D.  
501 Blake, P. Nava, N. Potrovitza, Engineering aspects of a molten salt heat transfer fluid in

- 502 a trough solar field, *Energy*. 29 (2004) 861–870. doi:10.1016/S0360-5442(03)00191-9.
- 503 [6] R.I. Olivares, The thermal stability of molten nitrite/nitrates salt for solar thermal energy  
504 storage in different atmospheres, *Sol. Energy*. 86 (2012) 2576–2583.  
505 doi:10.1016/j.solener.2012.05.025.
- 506 [7] C.S. Turchi, J. Vidal, M. Bauer, Molten salt power towers operating at 600–650 °C: Salt  
507 selection and cost benefits, *Sol. Energy*. 164 (2018) 38–46.  
508 doi:10.1016/j.solener.2018.01.063.
- 509 [8] X. Chen, Y. ting Wu, L. di Zhang, X. Wang, C. fang Ma, Experimental study on the  
510 specific heat and stability of molten salt nanofluids prepared by high-temperature  
511 melting, *Sol. Energy Mater. Sol. Cells*. 176 (2018) 42–48.  
512 doi:10.1016/j.solmat.2017.11.021.
- 513 [9] S. Omran, P. Heggs, Y. Ding, The influence of moisture content on the evaluation of  
514 latent heat of molten salts used for thermal energy storage applications, *Energy Procedia*.  
515 46 (2014) 317–323. doi:10.1016/j.egypro.2014.01.188.
- 516 [10] G.J. Janz, C.B. Allen, N.P. Bansal, R.M. Murphy, R.P.T. Tomkins, *Physical Properties  
517 Data Compilations Relevant to Energy Storage. II. Molten Salts: Data on Single and  
518 Multi-Component Salt Systems*, (1978).
- 519 [11] Y. Takahashi, R. Sakamoto, M. Kamimoto, Heat capacities and latent heats of LiNO<sub>3</sub>,  
520 NaNO<sub>3</sub>, and KNO<sub>3</sub>, *Int. J. Thermophys.* 9 (1988) 1081–1090.  
521 doi:10.1007/BF01133275.
- 522 [12] Thomas Bauer, Nicole Pflieger, Nils Breidenbach, Markus Eck, Doerte Laing, Stefanie  
523 Kaesche. Material aspects of Solar Salt for sensible heat storage. *Applied Energy*, Vol  
524 111, pages1114-1119, 2013
- 525 [13] H.L. Zhang, J. Baeyens, J. Degreève, G. Cacères, Concentrated solar power plants:  
526 Review and design methodology, *Renew. Sustain. Energy Rev.* 22 (2013) 466–481.  
527 doi:10.1016/j.rser.2013.01.032.
- 528 [14] M. Zeki Yilmazoglu, Effects of the selection of heat transfer fluid and condenser type on  
529 the performance of a solar thermal power plant with technoeconomic approach, *Energy  
530 Convers. Manag.* 111 (2016) 271–278. doi:10.1016/j.enconman.2015.12.068.
- 531 [15] G.J. Kolb, C.K. Ho, T.R. Mancini, J.A. Gary, *Power Tower Technology Roadmap and  
532 cost reduction plan*, 2011. doi:10.2172/1011644.
- 533 [16] International Renewable Energy Agency (IRENA), *Renewable power generation costs in  
534 2014*, *Renew. Power Gener. Costs.* (2014) 1–8. doi:10.1007/SpringerReference\_7300.
- 535 [17] J. Hinkley, B. Curtin, J. Hayward, A. \Wonhas, R. Boyd, C. Grima, A. Tadros, R. Hall,  
536 K. Naicker, A. Mikhail, *Concentrating solar power – drivers and opportunities for cost-  
537 competitive electricity*, 2011. www.csiro.au.
- 538 [18] G. Cáceres, N. Arnique, A. Girard, J. Degreève, J. Baeyens, H.L. Zhang, *Performance of*

539 molten salt solar power towers in Chile, *J. Renew. Sustain. Energy*. 5 (2013) 053142.  
540 doi:10.1063/1.4826883.

541 [19] Donald C. Rennels, H.M. Hudson, *Pipe Flow: A Practical and Comprehensive Guide*,  
542 Wiley, 2012.

543 [20] D. Kearney, *Utility-scale Power Tower Solar Systems: Performance Acceptance Test*  
544 *Guidelines*, 2014.

545 [21] C.S. Turchi, M.J. Wagner, *POWER TOWER REFERENCE PLANT FOR COST*  
546 *MODELING WITH THE SYSTEM*, in: *WREF 2012 - 2012 World Renew. Energy*  
547 *Forum*, Denver, CO, USA, 2012: pp. 1–8.

548